Membrane curvature induced by Arf1-GTP is essential for vesicle formation

Rainer Beck*, Zhe Sun*, Frank Adolf, Chistoph Rutz, Jochen Bassler, Klemens Wild, Irmgard Sinning, Ed Hurt, Britta Brügger, Julien Béthune†, and Felix Wieland†

Biochemistry Center, Heidelberg University, Im Neuenheimer Feld 328, D-69120 Heidelberg, Germany

Communicated by James E. Rothman, Columbia University Medical Center, New York, NY, June 9, 2008 (received for review April 2, 2008)

The GTPase Arf1 is considered as a molecular switch that regulates binding and release of coat proteins that polymerize on membranes to form transport vesicles. Here, we show that Arf1-GTP induces positive membrane curvature and find that the small GTPase can dimerize dependent on GTP. Investigating a possible link between Arf dimerization and curvature formation, we isolated an Arf1 mutant that cannot dimerize. Although it was capable of exerting the classical role of Arf1 as a coat receptor, it could not mediate the formation of COPI vesicles from Golgi-membranes and was lethal when expressed in yeast. Strikingly, this mutant was not able to deform membranes, suggesting that GTP-induced dimerization of Arf1 is a critical step inducing membrane curvature during the formation of coated vesicles.

dimerization | biosynthetic membrane transport | GTPase

Small GTPases of the Ras superfamily are key regulators of many important cellular functions (1). They work as molecular switches that cycle between an inactive GDP-bound state and an active GTP-bound state. Activation occurs by the exchange of GDP to GTP, whereas inactivation is mediated by GTP hydrolysis. Effectors of GTP-binding proteins are defined as molecules that bind more tightly to the GTP-bound state, resulting in a biological function.

The small GTPase Arf1 is involved in the recruitment of coat protein complexes that polymerize on endomembranes to form transport vesicles (2, 3). Activated Arf1 is always membrane-associated because, in this conformation, its myristoylated N-terminal amphipatic α-helix is exposed, ensuring membrane anchorage (4). Because coat proteins can only bind to the active GTPase (5–7), Arf1 is a key regulator of vesicle coating and uncoating. Indeed, activation of Arf1 is a prerequisite for coat recruitment (8–10), and Arf1-mediated GTP hydrolysis is necessary for coat release (11, 12). Arf1-GTP is directly involved in the recruitment of coatomer (7, 8), the coat of COPI vesicles (13) and of the clathrin adaptor complexes AP-1 (10), AP-3 (9) and AP-4 (5). COPI-coated vesicles mediate protein and lipid transport within the early secretory pathway (14). Coatomer directly interacts with Arf1 through binding of several of its subunits in a GTP-dependent manner. We have reported evidence that more than one Arf1-GTP molecule may bind to one coatomer complex (15). This finding is in agreement with estimations of an Arf1-to-coatomer stoichiometry on COPI-coated vesicles of at least 3:1 (2, 16, 17). These observations suggest that Arf1, which like most other Ras-like GTPases is a monomer in its cytosolic form, may oligomerize upon activation on membranes. Here, we show that Arf1, when bound to GTP, in fact forms a dimer on the membrane and provide evidence that this dimerization is required to generate COPI vesicles. Interestingly, Arf1-GTP induces positive membrane curvature, as shown by tubulation of membrane sheets, whereas a nondimerizing Arf1-mutant lacks this activity.

Results and Discussion

GTP-Dependent Membrane Deformation by Arf1. In our attempt to understand the mechanism of vesicle budding at a molecular level and in the light of Arf1's homolog in the COPII pathway, Sar1p, inducing membrane deformation (18), we investigated whether Arf1-GTP has such a membrane activity. To this end, we made use of a light microscopic liposome tubulation assay, similar to that used by Roux *et al.* (19). A mix of Golgi-like lipids containing p23 lipopeptide (20, 21) was spotted on a glass surface and dried. After rehydration, lipid sheets were formed that could be observed by light microscopy. In our assay, the reaction partners ARNO [an exchange factor for Arfs (22)] and nucleotide are added, and the reaction is started by the addition of myristoylated Arf1. As shown in Fig. 1*A*, Arf1 indeed catalyzes the GTP-dependent formation of tubules from lipid bilayers. This effect is observed at concentrations of Arf1 (0.6 μg of protein/μg of lipids) similar to the concentration of F-BAR proteins that have been found to form tubules in this assay (23). In the absence of GTP, no tubules are formed (Fig. 1*B*). Note that the order of addition of reaction partners is interchangeable and yields the same result. Real-time recordings of these assays allow an easier observation of the tubulation by Arf1-GTP and are found in supporting information (SI) Movies S1 and S2. With these findings, we propose that activated Arf1 has, in addition to its GTP-switch function, a role in inducing membrane curvature in the process of budding of a transport vesicle.

GTP-Dependent Dimerization of ARF1. Many of the proteins that directly affect membrane curvature are dimeric or have multiple domains (24, 25). Because we had indications that Arf1 may dimerize (15), we analyzed this possibility in initial experiments described in (Fig. S1), where cross-link experiments are shown with *in vitro* translated [^{35}S]Methionine-labeled Arf1 bound to Golgi membranes. These findings revealed a GTP-dependent band at a migration expected for a dimer of the small GTPase. To further test for dimerization, recombinant myristoylated Arf1 was incubated with protein-free liposomes, GTPγS, and chemical cross-linkers. After isolation of the liposome-bound material and analysis by Western blotting, a cross-linker-dependent ≈40-kDa band was observed with the homobifunctional thiol reagent Bis-maleimido-hexane (BMH) (0.5 mM) (Fig. 2, lane 4), and with a heterobifunctional reagent (active with thiol and amino groups) *N*-(ε-maleimido-caproyloxy)-*N*-hydroxy-succinimide ester (EMCS) (0.5 mM) (Fig. 2, lane 2). Thus, Arf1 efficiently dimerizes on membranes dependent on GTP and in the absence of any additional factors.

Model for an Arf1-GTP Dimer. To identify the dimerization interface within Arf1, material from the bands in Fig. 2 was digested

Author contributions: R.B., Z.S., I.S., E.H., B.B., J. Bethune, and F.W. designed research; R.B., Z.S., F.A., C.R., J. Bassler, and K.W. performed research; B.B., J. Bethune, and F.W. analyzed data; and R.B., J. Bethune, and F.W. wrote the paper.

The authors declare no conflict of interest.

*R.B. and Z.S. contributed equally to this work.

†To whom correspondence may be addressed. E-mail: julien.bethune@fmi.ch or felix.wieland@bzh.uni-heidelberg.de.

This article contains supporting information online at www.pnas.org/cgi/content/full/0805182105/DCSupplemental.

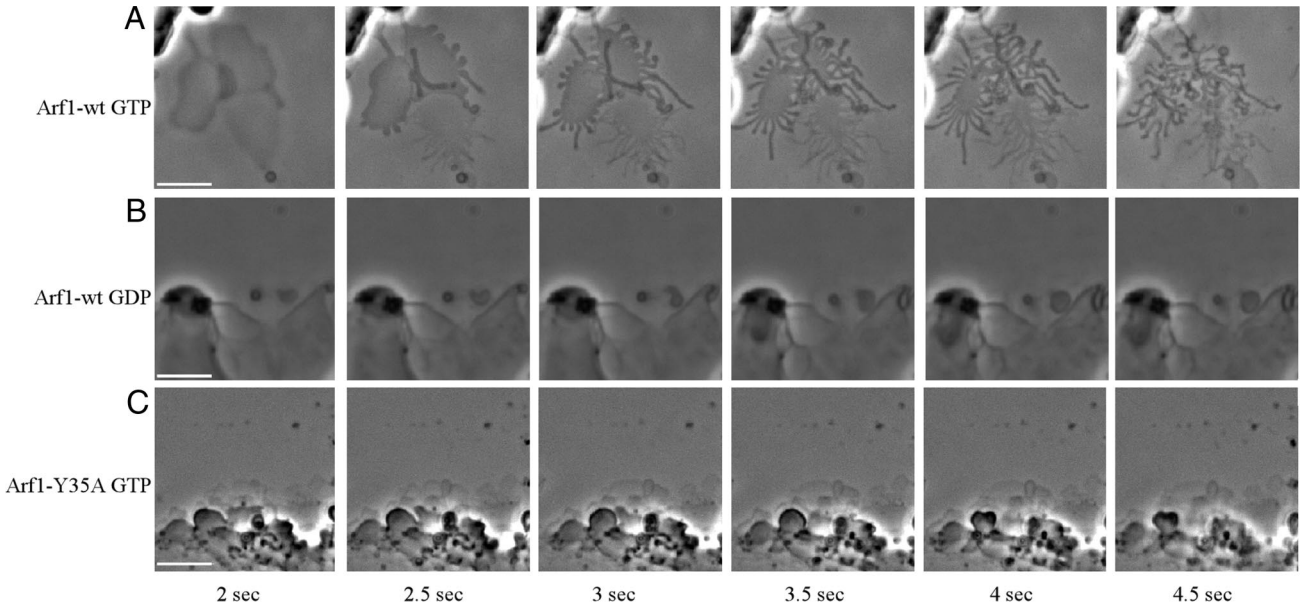

Fig. 1. Arf1-mediated tubulation of synthetic lipid sheets. Lipids containing p23 lipopeptide were spotted on a glass surface and hydrated with buffer containing either GTP or GTP and the exchange factor ARNO (50 nM). After addition of myristoylated Arf1-GDP (1 μM), the lipid surface was observed by light microscopy. Shown are the reactions in the presence of Arf1-wt with GTP (*A*), Arf1-wt with GDP (*B*), and Arf1-Y35A with GTP (*C*). Scale bars, 5 μm.

with trypsin and analyzed by mass spectrometry. Without cross-linker, peptides covering the complete Arf1 sequence were detected, except its N-terminal myristoylated α-helix. In contrast, two peptides (amino acids 31–36 and 152–178) were missing in the isolated EMCS-cross-linked Arf1 dimer (Fig. S2). These two regions within the Arf1 sequence are thus probably involved in the dimerization interface. Arf1 possesses a single cysteine residue (Cys-159), which is part of the missing C-terminal peptide. Therefore, we used homobifunctional cysteine cross-linkers of varying spacer lengths to measure the distance between two Arf1 molecules forming a dimer. Strikingly, cross-linking of two Arf1 molecules is optimal with a spacer length of 16 Å and decreases when the length is shorter or longer (Fig. 3*A*). To verify whether an Arf1 dimer with this interface would comply with the known properties of the small GTPase, we modeled a possible dimer based on the crystal structure available with the highest resolution of a truncated soluble form of Arf1-GTP, $N_{\Delta 17}$Arf1 (PDB ID code 1O3Y) (26). To this end, the observed optimal distance of the two single Cys-sulfur atoms was used, and the following constraints: The N-terminal α-helices of both Arf1 molecules must contact the membrane, established

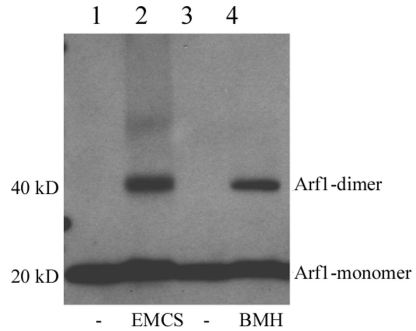

Fig. 2. Arf1 dimerizes on protein-free liposomes. Protein-free liposomes were incubated with full-length myristoylated Arf1, GTP, and the cross-linkers EMCS (lane 2) or BMH (lane 4) as indicated. After centrifugation, the liposome-bound material was analyzed by Western blotting with an anti-Arf1 antibody.

protein–protein interaction sites (involving coatomer or ArfGAP1) should be accessible, the dimerization interface should be comprised of at least parts of both peptides identified by mass spectrometry, the interactions should be energetically favorable, and sterical clashes should not occur.

This yielded a homodimeric model of full-length membrane-associated Arf1-GTP (Fig. 3*B*), which is symmetric and includes an intermolecular β-sheet completion formed by the interswitch regions. The crystal structures of $N_{\Delta 17}$Arf1-GTP and full-length nonmyristoylated Arf1-GDP also show a dimer (26, 27), although these proteins are found as monomers in solution by gel filtration (data not shown). In these crystals, the dimerization interfaces are different from our model of a full-length Arf1-GTP dimer and would not allow the cross-links we observe (Figs. 2 and 3). Often, proteins crystallize in oligomeric forms that are not physiologically relevant (crystallographic oligomers). A structure of full-length Arf1-GTP is not available because the protein is insoluble in the absence of membranes. This is of importance because the membrane accommodates the hydrophobic regions of Arf1 that are exposed in its GTP state and may participate in the dimerization by orienting and stabilizing a biologically relevant dimeric structure (4).

Characterization of an Arf1 Variant That Cannot Dimerize. According to our model, single amino acids within and around the putative interface were exchanged for alanine, and the resulting Arf1 variants were probed for their ability to dimerize. A Arf1-Y35A mutant has lost the ability to dimerize, as analyzed by a cross-link assay of Golgi-bound Arf1 proteins (Fig. 4). The mutated protein is capable of nucleotide exchange, as assessed by ^{3}H-GTP-exchange assays with Golgi membranes. The ability of Arf1-Y35A to exert the classical GTP switch for coat recruitment (28) was investigated by static light scattering (SLS) experiments on liposomes, performed similar to those in ref. 21 and by analyzing coat recruitment (as shown for coatomer and adaptin-1) to Golgi membranes. These data are provided in Figs. S3–S5. In Fig. S3, the nucleotide exchange activity of Arf1-Y35A was assayed and found to be $\approx$70% of Arf1-wt. Binding studies with Golgi-enriched membranes revealed nucleotide-specific recruitment of both coatomer and adaptin-1 with Arf1-wt and the mutant,

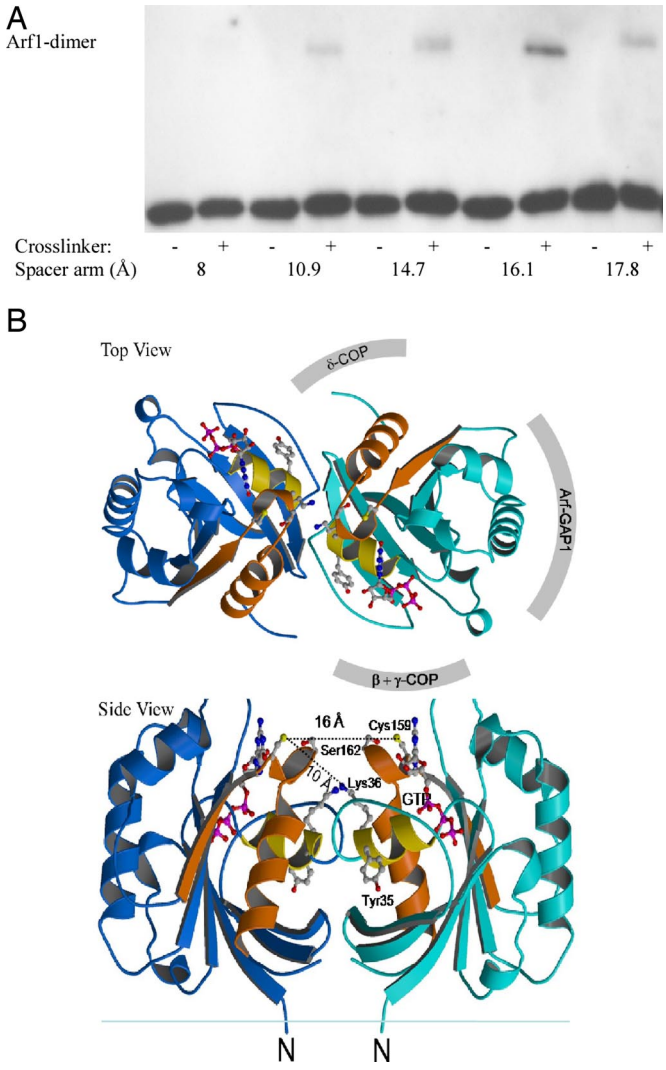

Fig. 3. Biochemical characterization and modeling of an Arf1-GTP dimer. (*A*) The distance between the cysteines in an Arf1 dimer is optimal at 16Å. Protein-free liposomes were incubated with full-length myristoylated Arf1, GTPγS, and homobifunctional thiol-reactive cross-linkers of increasing spacer length as indicated (see *Materials and Methods*). The liposome-bound material was analyzed by Western blotting with an anti-Arf1 antibody. (*B*) Model of an Arf1 dimer. Shown are models of the Arf1-GTP dimer in a view toward the membrane (*Upper*) and from the membrane plane (*Lower*). The model is based on the crystal structure of monomeric Arf1-GTP (PDB ID code 1O3Y) and the constraints as described in the text. The binding site of the Arf-GAP1 catalytic domain and mapped coatomer interactions are shown schematically for one monomer. The two missing cross-linked peptides from the mass spectrometry experiment are colored in yellow (31–36) and orange (152–178), and the critical tyrosyl residue in position 35, whose mutation to alanin results in a strong dimerization phenotype, is indicated. The cross-linked residues are connected by dashed lines, and their distances are indicated (the distance between Cys-159 and Lys-36 in the model is 10 Å, in accordance with the distance of the functional groups within the cross-linker EMCS). The interface coincides with the binding site of the N-terminal helix in Arf1-GDP and includes an intermolecular β-sheet completion formed by the exposed inter-switch regions of Arf1-GTP.

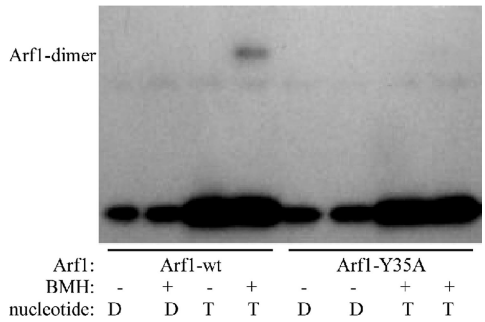

Fig. 4. Dimerization assay on Golgi membranes. Golgi-enriched membranes from rat liver were incubated with full-length myristoylated Arf1-wt, Arf1-Y35A, and GTPγS, and after recovery of membranes by centrifugation, the cross-linker BMH was added as described in *Materials and Methods*. Membrane-bound material was analyzed by Western blotting with an anti-Arf1 antibody.

further underlining that Arf1-Y35A is not compromised with regard to its established function in coat recruitment (Fig. S4). Furthermore, SLS studies showed that Arf1-Y35A is able to complete a cycle of coat recruitment and release, mediated by the nucleotide exchange factor ARNO and the GTPase-activating protein ArfGAP1. Interestingly, as opposed to Golgi-membranes, in this liposomal system the nucleotide exchange on the mutant seems to depend on coatomer. Overall, in this assay, a complete cycle of coat recruitment and release is mediated by Arf1-Y35A with an efficiency of ≈20% for the wild-type protein (Fig. S5). Finally, the localization of Arf1-Y35A *in vivo* was analyzed by confocal microscopy of cells expressing YFP-tagged Arf1 constructs. Mutant Arf1-Y35A showed a typical Golgi staining comparable with that of the wild-type protein (Fig. S6), although more cytosolic background staining was observed, probably reflecting the mutant's reduced activity compared with Arf1-wt (as shown in Figs. S3 and S5). Taken together, these data demonstrate that the Arf1-Y35A is functional in exerting the GTP-switch reaction, and, apart from not dimerizing, is similar to wild-type Arf1.

Lack of Function of Arf1Y35A Analyzed *in Vivo* and *in Vitro*. Yeast and mammalian Arf1 are 77% identical and functionally redundant (29), and the amino acid residue Y35 is conserved. Thus, to test the physiological significance of this mutation *in vivo*, we expressed the point mutant in *Saccharomyces cerevisiae*. Because in yeast yArf1 and yArf2 are 96% identical and are functionally redundant (30), plasmids expressing y*Arf1* and *yArf1-Y35A* were transformed into an *arf1*Δ *arf2*Δ deletion strain complemented by a pURA3 yArf1 plasmid (31). To test the growth behavior of the mutant, transformants were forced to lose the URA-plasmid by spotting on synthetic dextrose complete plates plus 5-fluorooratic acid monohydrate (SDC+FOA). Whereas the wild type was able to complement the yeast deletion strain, the *arf1-Y35A* mutation led to lethality at all tested temperatures (23°C, 30°C, and 37°C) (Fig. 5*A* and data not shown). Overexpression of *arf1-Y35A* by the Gal1 promoter had no dominant negative phenotype in a yeast wild-type strain (Fig. S7). Likewise, GAL1 overexpression of Arf1-Y35A did not rescue the effect of *arf1-wt* deletion, as shown in Fig. S7. Taken together, these experiments strongly indicate that dimerization is essential for the function of Arf1. Because Arf1 is involved in the recruitment of numerous coat complexes and notably coatomer, the COPI coat whose disruption is lethal in yeast (32), a potential role for the dimerization of Arf1 in the formation of COPI vesicles was investigated. To this end, we tested the point mutant in an *in vitro* budding assay where Arf1 and coatomer are incubated with GTP and Golgi membranes to induce COPI vesicle formation (33) (see *Materials and Methods*). The vesicles were then purified from the donor membranes by sucrose density gradient centrifugation. A typical result is shown in Fig. 5*B*. Whereas Arf1-wt yields strong signals in the vesicle-containing interface between 45% and 37.5% sucrose, indicated by the presence of Western blot signals for coatomer subunit δ-COP and the membrane

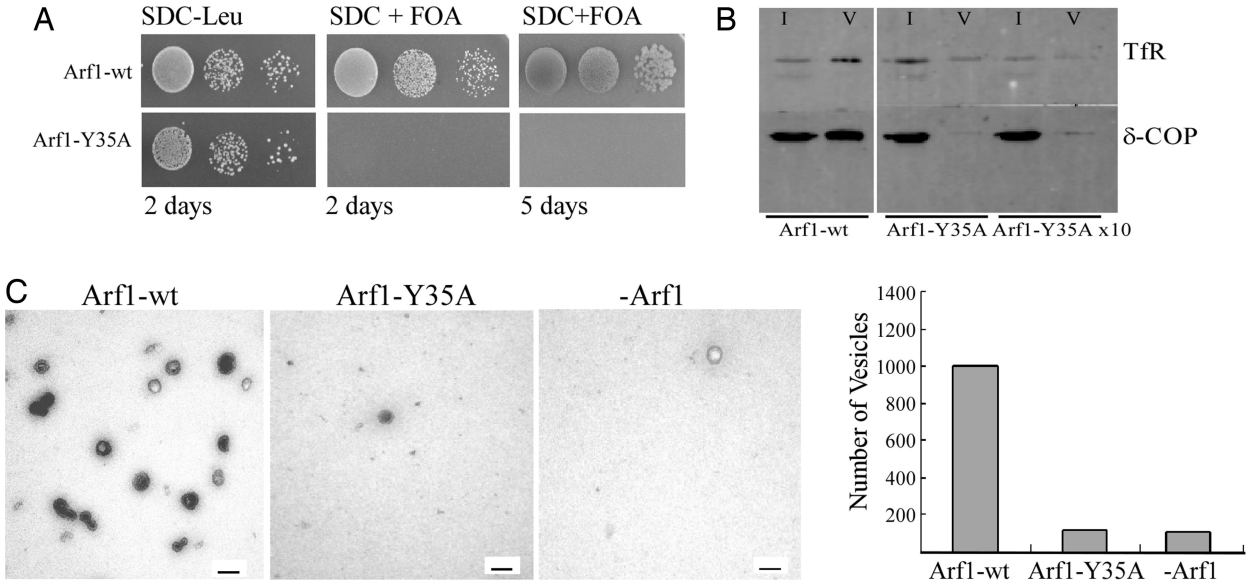

Fig. 5. The non dimerizing mutant Arf1-Y35A is lethal in yeast and does not support COPI-vesicle formation *in vitro*. (*A*) *In vivo* analysis of Arf1 mutants in yeast. Yeast strain NYY539 (*arf1*Δ, *arf2*Δ, *pURA3-Arf1*) was transformed with pRS315-Arf1, pRS315-arf1-S162A, and pRS315-arf1-Y35A. Transformants were spotted in 10^{-1} dilution series on SDC+FOA. Pictures were taken after 2 days or 5 days of incubation at 30°C. (*B*) *In vitro* formation of COPI vesicles in the presence of monomeric or dimeric Arf1. Golgi-enriched membranes were pretreated with 250 mM KCl and incubated with purified constituents of the COPI machinery, such as Arf1-wt or the monomeric mutant Y35A, and rabbit liver coatomer and GTP. COPI-coated vesicles were purified by sucrose density gradient centrifugation. For each sample, 5% of total input (I), and 50% of the purified vesicles (V) were analyzed by SDS/PAGE and Western blotting using antibodies against the coatomer subunit δ-COP and the transmembrane protein transferrin receptor (TfR). (*C*) Quantification of vesicle formation in the presence of monomeric or dimeric Arf1. Vesicles were generated either as described in *Materials and Methods* or after isopycnic density gradient centrifugation (33), followed by negative staining electron microscopy. Twenty meshes each of the samples were randomly chosen and the number of vesicles counted.

protein transferrin receptor (TfR) in lane 2, an identical amount of Arf1-Y35A does not give rise to significant signals (Fig. 5*B*, lane 4). Because the mutated protein has reduced coating activity in the SLS experiments, we increased the amount of input Arf1-Y35A by a factor of 10. Again, no significant signals were observed in the respective interface (Fig. 5*B*, lane 6). Vesicle formation was further analyzed by negative stain electron microscopy of fractions isolated by isopycnic sucrose density gradient centrifugation as described in ref. 33. As a result, a homogeneous population of vesicles is found in samples with Arf1-wt, whereas only sporadic vesicles are observed with Arf1-Y35A (Fig. 5*C*). Quantification of these experiments revealed an amount of vesicles obtained with Arf1-Y35A that did not exceed the numbers obtained by residual endogenous Arf1. Altogether, these experiments indicated that dimerization of Arf1-GTP is necessary for the formation of COPI vesicles and is critical at a step distinct from coatomer recruitment.

Our finding that dimerization is not critical for coatomer recruitment but is required for vesicle formation indicates that dimeric Arf1 plays an as yet unknown role in vesicle formation, possibly related to the membrane deformation activity reported in this work. To challenge this hypothesis, the ability of Arf1-Y35A to induce membrane deformation was assessed. Strikingly, the Arf1 mutant Y35A does not catalyze tubule formation (Fig. 1*C*). Real-time imaging of this condition is appended in Movie S3.

We have shown here that when bound to GTP, Arf1 has a membrane tubulation activity. Upon activation, the small GTPase undergoes a conformational change, resulting in the protrusion of its N-terminally myristoylated and amphiphilic α-helix, which is generally thought to be accommodated in the donor membrane (4). In a similar way, the amphipatic α-helix of the small GTPase Sar1p, involved in COPII vesicle formation, was reported to insert into and cause deformation of the membrane (18). Because, apart from dimerization, Arf1-Y35A behaves like the wild type, we assume that in the monomeric mutant this α-helix is also inserted in membranes. It appears then that it is the insertion in a lipid leaflet of a pair of amphipatic stretches that results in the membrane tubulation activity induced by Arf1. Strikingly, synaptotagmin also induces membrane deformation by inserting a pair of C2 domains in membranes and loses this activity if one of the two domains is removed (24). Similarly, dimerization has been proposed to regulate the membrane deformation activity of endophilin (34) and of an EHD-ATPase (35). Therefore, oligomerization of membrane-deforming protein domains seems to regulate their effect.

In the context of vesicle formation, the interplay between Arf1 dimerization and multivalent binding to coatomer might even harbor a further mechanistic step. Indeed, as a monomeric activated Arf1 (mutant Y35A, Fig. S4) can bind to and recruit coatomer to membranes, and as multiple Arf1s are found per one coatomer in COPI vesicles (2, 15–17), activated Arf1 dimers could be cross-linked by the recruited coat complexes. This cross-linkage would result in the localized insertion of multiple pairs of amphipatic stretches, leading to a high membrane-destabilization activity under a forming coat lattice, promoting the formation of a bud. Interestingly, in such a model, the final shape of the nascent bud would most probably be governed by the coat proteins, because they sit directly above the localized and concentrated membrane destabilization foci mediated by dimers of Arf1.

Together, our results suggest a mechanism of vesicle biogenesis that critically depends on bending of membranes induced by dimeric Arf1. This revisits the current paradigm for the role of Arf1 in the formation of transport vesicles because the small GTPase was solely seen as a molecular switch that regulates the recruitment of coat proteins to membranes.

Materials and Methods

Antibodies. For Western blot analysis, the polyclonal rabbit anti-peptide antibodies 891 (anti-β′-COP), 877 (anti-δ-COP), HAC344 (anti-p23), and C1 (anti-Arf1) were used (36–39). For immunostaining, anti-Giantin was used (40).

Proteins. Point mutants of Arf1 were generated by site directed mutagenesis. N-myristoylated human Arf1-wt was expressed and purified from *Escherichia coli* (41). Arf1-Y35A was, after cell lysis and ultracentrifugation, subjected to a 35% ammonium sulfate precipitation, centrifuged, and the supernatant, bound to a phenylsepharose HP column (Amersham Pharmacia Biotech), was developed with a descending gradient from 35% to 0% ammonium sulfate in 20 mM Tris·HCl buffer pH 8.0, 1 mM $MgCl_2$, at room temperature (RT). Eluted fractions were analyzed by immunoblotting with anti-Arf1 antibody, pooled and concentrated in spin column filters with a 10-kDa cutoff (Milipore), and subsequently purified by gel filtration on a superdex-75. Fractions of interest were pooled and concentrated. Coatomer was purified from rabbit liver (42). His-tagged ARNO was expressed in *E. coli* and purified by Ni-NTA chromatography.

Preparation of Golgi Membranes. Golgi membranes were purified from HeLa cells (43) or rat liver homogenates (44).

Preparation of Liposomes. All phospholipids and cholesterol were purchased from Avanti Polar Lipids except for phosphatidic acid, which was from Sigma. Lipids were derived from natural sources (45).

Golgi-like liposomes were prepared, as described in ref. 39, containing 1 mol% phosphatidylinositol-4,5-bisphosphate ($PI(4,5)P_2$) and 2 mol% p23 lipopeptide, which was synthesized as described in ref. 20. Size selection was performed by extrusion through 100-nm polycarbonate filter membranes (Avestin).

Golgi Binding Assay. Binding of Arf1 and coatomer to HeLa and rat liver Golgi membranes was performed as described in ref. 7. Briefly, after a 3-min incubation at 37°C of 10 μg of HeLa Golgi membranes with 0.6 μg of either Arf1-wt or Arf1-Y35A in the presence of 50 μM nucleotide (GDPβS or GTPγS) in assay buffer [25 mM Hepes-KOH (pH 7.2), 2.5 mM magnesium acetate, 20 mM KCl, ovalbumin (1 mg/ml), 1 mM DTT, and 200 mM sucrose], 2 μg of rabbit liver coatomer was added to achieve an end volume of 50 μl. After an additional 15-min incubation, Golgi membranes were pelleted by loading the sample onto a 300-μl cushion of 15% sucrose (wt/vol), followed by a 30-min centrifugation at 16,000 $\times$ *g* (4°C). Pellets were resuspended in SDS sample buffer and, after separation by SDS/PAGE, analyzed by Western blotting with antibodies against Arf1 and COP subunits.

Chemical Cross-Linking. For analysis of Arf1 dimers, the Golgi binding assay was performed as described above. After binding, pelleted membranes were resuspended in PBS (e.g., 12.5 μg of membranes in 20 μl) and 0.5 mM cross-linker, and either EMCS or BMH (Pierce) was added from a 10 mM solution in DMSO. The reaction mixture was incubated for 1 h at RT, and then SDS sample buffer was added. Samples were analyzed by SDS/PAGE and Western blotting with an antibody against Arf1 and by mass spectrometry.

Dimerization Assay with Protein-Free Liposomes. To analyze dimerization of Arf1-wt and Arf1-Y35A on liposomes, Arf1 proteins were incubated with liposomes containing 2 mol% p23 lipopeptide and 1 mol% $PI(4,5)P_2$ (200 nmol of total lipids) with 33 μg (0.1 μM) of coatomer, 10 μg (1 μM) of Arf1, 2 μg (0.1 μM) of ARNO, and 100 μM GTPγS or GDPβS at 37°C for 40 min in 500 μl of PBS. Thereafter, the sucrose concentration was adjusted to 52% (wt/wt) by the addition of 65% (wt/wt) sucrose in PBS. The sample was transferred to a SW60 tube and overlaid with 750 μl of 42% (wt/wt) sucrose in PBS and 750 μl of 10% (wt/wt) sucrose in PBS. Centrifugation was performed at 20,000 $\times$ *g* for 2.5 h (4°C). Typically, liposomes are visible as an opalescent band at the interface between 42% and 10% sucrose. The liposome fractions were collected and membrane-bound Arf1 was analyzed by Western blotting with an antibody against Arf1. Incubation with cross-linker was as that described for Golgi membranes. Alternatively, Golgi-like liposomes without lipopeptide were incubated with Arf1-wt, and nucleotide exchange was performed by addition of EDTA, GTPγS, and thereafter $MgCl_2$, as described in ref. 41, followed by chemical cross-linking.

Formation of COPI Vesicles *in Vitro*. COPI vesicle budding assays with rat-liver Golgi membranes and Arf1 (Arf1-wt or Arf1-Y35A,) were performed as described in ref. 33. For the rapid generation of COPI vesicles in the presence of GTP, the method was modified: 200 μg of rat-liver Golgi membranes (pretreated with 500 mM KCl), 10 μg of myristoylated Arf1 protein, and 25 μg of coatomer were incubated for 10 min at 37°C in a total volume of 250 μl in assay buffer [25 mM Hepes-KOH (pH 7.4), 2.5 mM magnesium acetate, 50 mM KCl, 1.2 mM GTP, 300 mM sucrose, and 0.25 mM DTT], and 1% of the input was taken for Western blot analysis. The sample was subjected to 250 mM KCl to dissociate tethered COPI vesicles from the donor Golgi membranes, which were pelleted by a 10-min centrifugation at 16,000 $\times$ *g* at 4°C. The supernatant, containing COPI vesicles, was laid on top of two sucrose cushions in a Beckman SW55-mini tube of 37.5% (50 μl) and 45% (5 μl) sucrose. After centrifugation for 50 min at 100,000 $\times$ *g*, the vesicles were collected at the 45/37.5% sucrose interphase and the collected material was analyzed by Western blotting, negative staining electron microscopy, and electrospray ionization tandem mass spectrometry to assess the lipid content.

Complementation Assays in Yeast. The yeast strain NYY539 (arf1Δ, arf2Δ, pURA3-Arf1) was kindly provided by A. Nakano (RIKEN, Saitama, Japan) (31). pRS315-Arf1-wt and pRS315-arf1-Y35A were generated by using standard procedures and transformed into NYY539. The cells were incubated at 23°C, 30°C, and 37°C for various times and transformants were spotted on SDC+FOA.

Arf1-Induced Tubulation of Membrane Sheets. A system similar to that described in ref. 19 was used. A chamber of approximately 30 μl was built between two microscope slides with two layers of parafilm as a spacer. Golgi-like lipids containing 1 mol% $PI(4,5)P_2$, and 2 mol% p23 lipopeptide (20) were spotted on the glass surface, and the solvent (CH_3Cl) was evaporated. The lipids were hydrated in the presence of nucleotide with 20 μl of assay buffer [25 mM Hepes-KOH (pH 7.4), 150 mM KCl, 1 mM DTT, 1 mM GTP or GDP]. Then, protein samples were sequentially added at the concentrations indicated in the legend of Fig. 1, and membrane morphology was observed in a phase contrast light microscope. Real-time recordings are available in Movies S1–S3.

ACKNOWLEDGMENTS. We thank A. Nakamo and K. Sato for the yeast strain NYY539–1; Rainer Duden and Irina Majoul for the Arf1-YFP plasmid; Andrea Hellwig and Hilmar Bading for EM support; Volker Haucke, Michael Brunner, Walter Nickel, Harvey MacMahon, and Alfred Wittinghofer for critical comments; and Dr. J. Lechner for mass spectrometric characterization of proteins. This work was supported by German Research Council Grant SFB 638, A10.

1. Vetter IR, Wittinghofer A (2001) The guanine nucleotide-binding switch in three dimensions. *Science* 294:1299–1304.
2. Serafini T, *et al.* (1991) ADP-ribosylation factor is a subunit of the coat of Golgi-derived COP-coated vesicles: A novel role for a GTP-binding protein. *Cell* 67:239–253.
3. D'Souza-Schorey C, Chavrier P (2006) ARF proteins: Roles in membrane traffic and beyond. *Nat Rev Mol Cell Biol* 7:347–358.
4. Antonny B, Beraud-Dufour S, Chardin P, Chabre M (1997) N-terminal hydrophobic residues of the G protein ADP-ribosylation factor-1 insert into membrane phospholipids upon GDP to GTP exchange. *Biochemistry* 36:4675–4684.
5. Boehm M, Aguilar RC, Bonifacino JS (2001) Functional and physical interactions of the adaptor protein complex AP-4 with ADP-ribosylation factors (ARFs). *EMBO J* 20:6265–6276.
6. Austin C, Boehm M, Tooze SA (2002) Site-specific cross-linking reveals a differential direct interaction of class 1, 2, and 3 ADP-ribosylation factors with adaptor protein complexes 1 and 3. *Biochemistry* 41:4669–4677.
7. Zhao L, *et al.* (1997) Direct and GTP-dependent interaction of ADP ribosylation factor 1 with coatomer subunit beta. *Proc Natl Acad Sci USA* 94:4418–4423.
8. Donaldson JG, Cassel D, Kahn RA, Klausner RD (1992) ADP-ribosylation factor, a small GTP-binding protein, is required for binding of the coatomer protein beta-COP to Golgi membranes. *Proc Natl Acad Sci USA* 89:6408–6412.
9. Ooi CE, Dell'Angelica EC, Bonifacino JS (1998) ADP-ribosylation factor 1 (ARF1) regulates recruitment of the AP-3 adaptor complex to membranes. *J Cell Biol* 142:391–402.
10. Stamnes MA, Rothman JE (1993) The binding of AP-1 clathrin adaptor particles to Golgi membranes requires ADP-ribosylation factor, a small GTP-binding protein. *Cell* 73:999–1005.
11. Tanigawa G, *et al.* (1993) Hydrolysis of bound GTP by ARF protein triggers uncoating of Golgi-derived COP-coated vesicles. *J Cell Biol* 123:1365–1371.
12. Zhu Y, Traub LM, Kornfeld S (1998) ADP-ribosylation factor 1 transiently activates high-affinity adaptor protein complex AP-1 binding sites on Golgi membranes. *Mol Biol Cell* 9:1323–1337.
13. Waters MG, Serafini T, Rothman JE (1991) 'Coatomer': A cytosolic protein complex containing subunits of non-clathrin-coated Golgi transport vesicles. *Nature* 349:248–251.
14. Lee MC, Miller EA, Goldberg J, Orci L, Schekman R (2004) Bi-directional protein transport between the ER and Golgi. *Annu Rev Cell Dev Biol* 20:87–123.
15. Sun Z, *et al.* (2007) Multiple and stepwise interactions between coatomer and ADP-ribosylation factor-1 (Arf1)-GTP. *Traffic* (*Copenhagen*, *Denmark*) 8:582–593.
16. Sohn K, *et al.* (1996) A major transmembrane protein of Golgi-derived COPI-coated vesicles involved in coatomer binding. *J Cell Biol* 135:1239–1248.
17. Helms JB, Palmer DJ, Rothman JE (1993) Two distinct populations of ARF bound to Golgi membranes. *J Cell Biol* 121:751–760.
18. Lee MC, *et al.* (2005) Sar1p N-terminal helix initiates membrane curvature and completes the fission of a COPII vesicle. *Cell* 122:605–617.
19. Roux A, Uyhazi K, Frost A, De Camilli P (2006) GTP-dependent twisting of dynamin implicates constriction and tension in membrane fission. *Nature* 441:528–531.

20. Bremser M, *et al.* (1999) Coupling of coat assembly and vesicle budding to packaging of putative cargo receptors. *Cell* 96:495–506.
21. Bigay J, Antonny B (2005) Real-time assays for the assembly-disassembly cycle of COP coats on liposomes of defined size. *Meth Enzymol* 404:95–107.
22. Chardin P, *et al.* (1996) A human exchange factor for ARF contains Sec7- and pleckstrin-homology domains. *Nature* 384:481–484.
23. Frost A, *et al.* (2008) Structural basis of membrane invagination by F-BAR domains. *Cell* 132:807–817.
24. Martens S, Kozlov MM, McMahon HT (2007) How synaptotagmin promotes membrane fusion. *Science* 316:1205–1208.
25. Peter BJ, *et al.* (2004) BAR domains as sensors of membrane curvature: The amphiphysin BAR structure. *Science* 303:495–499.
26. Shiba T, *et al.* (2003) Molecular mechanism of membrane recruitment of GGA by ARF in lysosomal protein transport. *Nat Struct Biol* 10:386–393.
27. Amor JC, Harrison DH, Kahn RA, Ringe D (1994) Structure of the human ADP-ribosylation factor 1 complexed with GDP. *Nature* 372:704–708.
28. Bethune J, Wieland F, Moelleken J (2006) COPI-mediated transport. *J Membr Biol* 211:65–79.
29. Kahn RA, Kern FG, Clark J, Gelmann EP, Rulka C (1991) Human ADP-ribosylation factors. A functionally conserved family of GTP-binding proteins. *J Biol Chem* 266:2606–2614.
30. Stearns T, Kahn RA, Botstein D, Hoyt MA (1990) ADP ribosylation factor is an essential protein in *Saccharomyces cerevisiae* and is encoded by two genes. *Mol Cell Biol* 10:6690–6699.
31. Takeuchi M, Ueda T, Yahara N, Nakano A (2002) Arf1 GTPase plays roles in the protein traffic between the endoplasmic reticulum and the Golgi apparatus in tobacco and Arabidopsis cultured cells. *Plant J* 31:499–515.
32. Hosobuchi M, Kreis T, Schekman R (1992) SEC21 is a gene required for ER to Golgi protein transport that encodes a subunit of a yeast coatomer. *Nature* 360:603–605.
33. Serafini T, *et al.* (1991) A coat subunit of Golgi-derived non-clathrin-coated vesicles with homology to the clathrin-coated vesicle coat protein beta-adaptin. *Nature* 349:215–220.
34. Gallop JL, *et al.* (2006) Mechanism of endophilin N-BAR domain-mediated membrane curvature. *EMBO J* 25:2898–2910.
35. Daumke O, *et al.* (2007) Architectural and mechanistic insights into an EHD ATPase involved in membrane remodelling. *Nature* 449:923–927.
36. Harter C, Draken E, Lottspeich F, Wieland FT (1993) Yeast coatomer contains a subunit homologous to mammalian β'-COP. *FEBS Lett* 332:71–73.
37. Faulstich D, *et al.* (1996) Architecture of coatomer: Molecular characterization of delta-COP and protein interactions within the complex. *J Cell Biol* 135:53–61.
38. Jenne N, Frey K, Brugger B, Wieland FT (2002) Oligomeric state and stoichiometry of p24 proteins in the early secretory pathway. *J Biol Chem* 277:46504–46511.
39. Reinhard C, Schweikert M, Wieland FT, Nickel W (2003) Functional reconstitution of COPI coat assembly and disassembly using chemically defined components. *Proc Natl Acad Sci USA* 100:8253–8257.
40. Seelig HP, Schranz P, Schroter H, Wiemann C, Renz M (1994) Macrogolgin—A new 376 kD Golgi complex outer membrane protein as target of antibodies in patients with rheumatic diseases and HIV infections. *J Autoimmun* 7:67–91.
41. Franco M, Chardin P, Chabre M, Paris S (1996) Myristoylation-facilitated binding of the G protein ARF1GDP to membrane phospholipids is required for its activation by a soluble nucleotide exchange factor. *J Biol Chem* 271:1573–1578.
42. Pavel J, Harter C, Wieland FT (1998) Reversible dissociation of coatomer: Functional characterization of a beta/delta-coat protein subcomplex. *Proc Natl Acad Sci USA* 95:2140–2145.
43. Clary DO, Rothman JE (1990) Purification of three related peripheral membrane proteins needed for vesicular transport. *J Biol Chem* 265:10109–10117.
44. Tabas I, Kornfeld S (1979) Purification and characterization of a rat liver Golgi alpha-mannosidase capable of processing asparagine-linked oligosaccharides. *J Biol Chem* 254:11655–11663.
45. Nickel W, Wieland FT (2001) Receptor-dependent formation of COPI-coated vesicles from chemically defined donor liposomes. *Meth Enzymol* 329:388–404.